



## Microstructural and lattice parameter study of as-cast and rapidly solidified NiAl intermetallic alloys with Cu additions

J. Colín<sup>a,b,\*</sup>, S. Serna<sup>c</sup>, B. Campillo<sup>a,d</sup>, O. Flores<sup>a</sup>, J. Juárez-Islas<sup>e</sup>

<sup>a</sup> Instituto de Ciencias Físicas, Universidad Nacional Autónoma de México, Av. Universidad s/n, Col. Chamilpa, C.P. 62210 Cuernavaca, Morelos, Mexico

<sup>b</sup> Facultad de Ciencias Químicas e Ingeniería, Universidad Autónoma del Estado de Morelos, Av. Universidad No. 1001, Col. Chamilpa, C.P. 62209 Cuernavaca, Morelos, Mexico

<sup>c</sup> Centro de Investigación en Ingeniería y Ciencias Aplicadas-UAEM, Av. Universidad 1001, C.P. 62210 Cuernavaca, Morelos, Mexico

<sup>d</sup> Facultad de Química-Universidad Nacional Autónoma de México, Depto. de Metalurgia, Circuito Exterior S/N, Cd. Universitaria, C.P. 04510 México DF, Mexico

<sup>e</sup> Instituto de Investigaciones en Materiales – Universidad Nacional Autónoma de México, Circuito Exterior S/N, Cd. Universitaria, C.P. 04510 México DF, Mexico

### ARTICLE INFO

#### Article history:

Received 22 August 2007

Received in revised form 21 February 2008

Accepted 8 March 2008

Available online 3 June 2008

#### Keywords:

A. Nickel aluminides, based on NiAl

B. Martensitic transformations

C. Phase identification

C. Rapid solidification processing

D. Site occupancy

### ABSTRACT

In the current paper, the effect of Cu additions to the NiAl intermetallic compound on the microstructure and lattice parameter of the  $\beta$ -Ni(Al,Cu) and  $\gamma'$ -(Ni,Cu)<sub>3</sub>Al phases was investigated. As-cast and rapidly solidified specimens were characterized using X-ray diffractometry, scanning and transmission electron microscopy techniques. Biphasic microstructures composed of the B2  $\beta$ -Ni(Al,Cu) and L1<sub>2</sub>  $\gamma'$ -(Ni,Cu)<sub>3</sub>Al phases were observed in both cases, except in the alloy with 50 at.% Ni, 30 at.% Al, and 20 at.% Cu, which exhibits a martensitic microstructure composed of needles of  $\gamma'$ -(Ni,Cu)<sub>3</sub>Al with L1<sub>0</sub> tetragonal structure in the as-rapidly solidified condition. Generally  $\gamma'$ -Ni<sub>3</sub>Al is reported as an L1<sub>2</sub> cubic phase and there are many documents concerning such a phase, however, there are few publications with regard to  $\gamma'$ -(Ni,Cu)<sub>3</sub>Al with tetragonal structure. In addition, the present experimental data confirm the Bozzolo's model on site occupancy of ternary additions to the B2 NiAl intermetallic compound.

© 2008 Published by Elsevier Ltd.

### 1. Introduction

NiAl and Ni<sub>3</sub>Al intermetallic compounds have long been recognized as potentially useful structural materials for high temperature applications. The great interest in these intermetallic systems is due to their important properties for technological applications, such as high melting temperature, comparatively low density, good oxidation resistance, increase in yield strength with increasing temperature and extreme hardness [1]. The main obstacle to nickel aluminides as potential materials for use at elevated temperatures is their low room temperature ductility and low fracture toughness, particularly the grain boundary embrittlement in their polycrystalline form. In order to develop nickel aluminides for structural applications, extensive work has been focused on improvement of their mechanical properties. Much work has been carried out in single-phase Ni<sub>3</sub>Al alloys with the L1<sub>2</sub> structure, and as a result, remarkable improvements in these areas have been achieved [2].

Single-phase NiAl with the B2 structure has also been studied [3] and it is now clear that brittleness is not an inherent feature of

the  $\beta$  phase, so the resulting crystal as well as polycrystal with very fine grain size exhibits a fair ductility [4]. However, until now a solid remedy for room temperature brittleness has not yet been proposed.

It has been reported [5–7] that the addition of elements such as Cu, Fe, Co and Ti, as phase and microstructure modifiers might affect the properties of the NiAl intermetallic compound in a beneficial way. Many studies have found that microstructural modifications of  $\beta$ -NiAl including the ductile  $\gamma'$ -Ni<sub>3</sub>Al phase resulted in remarkable enhancements of high temperature strength and room temperature ductility [8–10]. Recently, Kainuma et al. [11] reported a systematic examination of microstructural evolution in  $\beta$  (B2) and  $\gamma'$  (L1<sub>2</sub>) forming alloys based on the Ni–Al–Fe system. The formation of a microstructure consisting of internally micro-twinned  $\gamma'$  (L1<sub>2</sub>) lamellae within the  $\beta$  matrix of an Ni–25 at.%–Al–15 at.%–Fe alloy was observed. This microstructure resulted in significantly increased yield strength and ductility when compared with specimens possessing other  $\gamma'$  morphologies (such as Widmanstätten, blocky and fine non-twinned lamellar). Kainuma proposed that the internally micro-twinned  $\gamma'$  lamellae is formed by the following sequence of events in quenched and aged samples:

1. Starting from an internally micro-twinned L1<sub>0</sub> type martensitic microstructure, further ordering of the L1<sub>0</sub> martensite to Ni<sub>5</sub>Al<sub>3</sub> occurs.

\* Corresponding author. Instituto de Ciencias Físicas, Universidad Nacional Autónoma de México, Av. Universidad s/n, Col. Chamilpa, C.P. 62210 Cuernavaca, Morelos, Mexico. Tel.: +52 777 3297039/1786; fax: +52 777 3297039.

E-mail addresses: [jmcc27@hotmail.com](mailto:jmcc27@hotmail.com), [jcolin@fis.unam.mx](mailto:jcolin@fis.unam.mx) (J. Colín).

- The  $\text{Ni}_5\text{Al}_3$  phase partially disorders, forming  $\gamma'$  *in situ*, such that the resulting  $\gamma'$  lamellae inherit the internally micro-twinned lamellar morphology of the  $\text{L1}_0$  martensite.

Furthermore, Kainuma et al. claimed that the prior formation of the  $\text{Ni}_5\text{Al}_3$  phase is an essential prerequisite for the production of internally micro-twinned  $\gamma'$  lamellae.

The purpose of the current paper is therefore to report the appearance of a microstructure similar to that reported by Kainuma when Cu additions are made to the NiAl intermetallic compound, excepting that in the present case, the martensitic phase is the  $\gamma'$ - $(\text{Ni,Cu})_3\text{Al}$  with a tetragonal  $\text{L1}_0$  crystal structure. In addition, it is observed that the formation mechanism of the martensitic  $\gamma'$  phase is different from that reported by Kainuma in the Ni–Al–Fe system.

## 2. Experimental procedure

Three NiAl intermetallic alloys with Cu additions (Cu as macroalloying element) were prepared by melting mixtures of Al (99.98%), electrolytic Cu (99.98%) and Ni (99.98%), in a Leybold–Heraeus Mod. HV-264 vacuum induction furnace and graphite crucibles. The resulting alloys were re-melted into quartz crucibles and rapidly solidified by the impingement of the liquid stream onto a copper wheel rotating at 15 m/s under an Ar atmosphere. Melt-spun ribbons of about 75  $\mu\text{m}$  thickness, 0.5 cm width and 30 cm length were obtained.

The location of the alloys in the ternary Ni–Al–Cu phase diagram and the proposed chemical composition (at.%) are shown in Fig. 1 and Table 1, respectively.

All of the alloys were characterized in both stages, as-cast and rapid solidification using a Siemens D-500 X-ray diffractometer, SEM Jeol JSM 6400 and TEM Jeol 2100 microscopes.

## 3. Results and discussion

Table 1 shows both the proposed and the real chemical compositions of the alloys in at.%. As it can be seen the compositional deviation from the proposed compositions is less than 1% in the Ni content,  $\pm 4.5\%$  for Al content and  $\pm 4.7\%$  for the Cu content. Such deviation is considered negligible since the new compositions lie inside the  $\beta + \gamma'$  field which is of our interest.

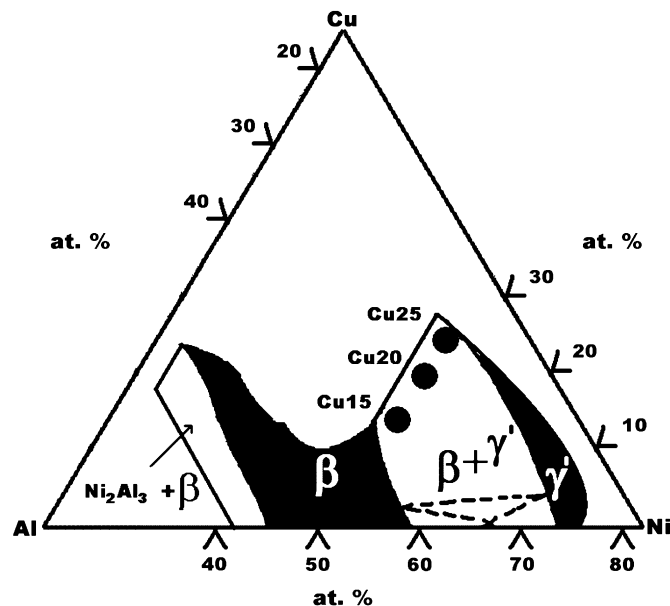


Fig. 1. Portion of the ternary Ni–Al–Cu phase diagram reported by Lipson and Bradley [12] showing the location of the alloys under study.

Table 1

Proposed and real chemical compositions (at.%) of the alloys

Alloy	Proposed			Real		
	Ni	Al	Cu	Ni	Al	Cu
Cu15	50	35	15	49.47	35.8	14.73
Cu20	50	30	20	49.24	28.15	22.60
Cu25	50	25	25	49.28	26.29	24.43

### 3.1. Microstructure

According to the data listed in Table 1 and the ternary Ni–Cu–Al phase diagram, all three alloys lie in the biphasic field formed by the  $\beta$ -Ni(Al,Cu) +  $\gamma'$ - $(\text{Ni,Cu})_3\text{Al}$  phases.

Figs. 2 and 3, show the microstructures observed in the alloys at the different conditions, as-cast and rapid solidification. Morphological differences between them can be seen. For example, Cu15, Cu20 and Cu25 alloys as-cast show polyphasic microstructures being columnar dendritic type for the Cu15 alloy and like-columnar dendritic type for the Cu25 alloy. On the other hand, the Cu20 alloy shows a morphologically like-martensitic microstructure. SEM observations and EDX microanalysis performed in the alloys show that the dendrites in the Cu15 as-cast alloy, shown in Fig. 2(a), are formed of  $\beta$ -Ni(Al,Cu) phase with the presence of a eutectic of the  $\beta$ -Ni(Al,Cu) +  $\gamma'$ - $(\text{Ni,Cu})_3\text{Al}$  type in the interdendritic spaces. In the same way, alloy Cu20, seen in Fig. 2(b), exhibits a like-martensitic microstructure formed by lengthened plates of  $\gamma'$ - $(\text{Ni,Cu})_3\text{Al}$  embedded into a matrix composed of  $\beta$ -Ni(Al,Cu) +  $\gamma'$ - $(\text{Ni,Cu})_3\text{Al}$ . Finally, the Cu25 alloy in Fig. 2(c) possesses a dendritic microstructure similar to that of the alloy Cu20. However, in the Cu25 alloy, there exist dendrites of  $\gamma'$  surrounded by a white phase which also was identified as  $\gamma'$ - $(\text{Ni,Cu})_3\text{Al}$ .

According to the X-ray diffraction patterns, the  $\gamma'$ - $(\text{Ni,Cu})_3\text{Al}$  phase with cubic  $\text{L1}_2$  ( $\gamma'_\text{C}$ ) and the  $\gamma'$ - $(\text{Ni,Cu})_3\text{Al}$  phase with tetragonal  $\text{L1}_0$  ( $\gamma'_\text{T}$ ) crystal structure exists in the Cu20 and Cu25 alloys, however the  $\gamma'_\text{T}$  phase was very difficult to detect and observe by TEM in the Cu20 alloy, and just a bit easier in the Cu25 alloy. The explanation is that in the Cu20 alloy the amount of  $\gamma'_\text{T}$  is rather small, whereas the amount of  $\gamma'_\text{T}$  in Cu25 alloy is higher. Fig. 4(a) and (b) shows TEM micrographs of the tetragonal  $\gamma'$ - $(\text{Ni,Cu})_3\text{Al}$  phase present in the Cu20 alloy and in the Cu25 alloy, respectively. In Fig. 4(a) it is clear that in the Cu20 alloy, the  $\gamma'_\text{T}$  phase exhibits like-plate shapes. Otherwise, in the Cu25 alloy shown in Fig. 4(b), the tetragonal  $\gamma'$ - $(\text{Ni,Cu})_3\text{Al}$  phase does not have like-plate morphology but a like-flake one, which apparently nucleates or forms in the edge of the dendrites, as seen in Fig. 2(c). In the same photo it can be seen that the  $\gamma'_\text{T}$  phase in some regions of the microstructure exhibits long shapes with certain parallelism, which suggests a preferential orientation. The presence of the  $\beta$ -Ni(Al,Cu) phase in the Cu25 alloy was neither observed nor detected by SEM and EDX, however, X-ray diffraction patterns show some peaks just as in the Cu20 alloy, indicating the presence of the  $\beta$ -Ni(Al,Cu) phase. The appearance of the  $\beta$ -Ni(Al,Cu) and  $\gamma'$ - $(\text{Ni,Cu})_3\text{Al}$  phases in these alloys is in good agreement with the Ni–Cu–Al ternary diagram reported by Lipson and Bradley [12]. However, the lack of observed or detected  $\beta$ -Ni(Al,Cu) phase by SEM and EDX suggests the possible occurrence of an extension of the solid solubility field of the  $\gamma'$  phase and the almost suppression of the  $\beta$  phase due to the relatively high solidification rate. The lost heat rate was 30  $^\circ\text{C}/\text{min}$  in the ingot compared to slowly cooled reported in the ternary phase diagram.

Concerning the alloys with rapid solidification (Fig. 3(a)–(c)), it can be seen that the Cu15 alloy exhibits a microstructure formed by polygonal grains of  $\beta$ -Ni(Al,Cu) as the major phase with a mean grain size of about 15  $\mu\text{m}$ . The presence of traces of  $\gamma'_\text{T}$  phase was also detected. In the same way, the Cu20 alloy shows polygonal grains about 15  $\mu\text{m}$  in size with  $\gamma'_\text{T}$  martensite needles inside the

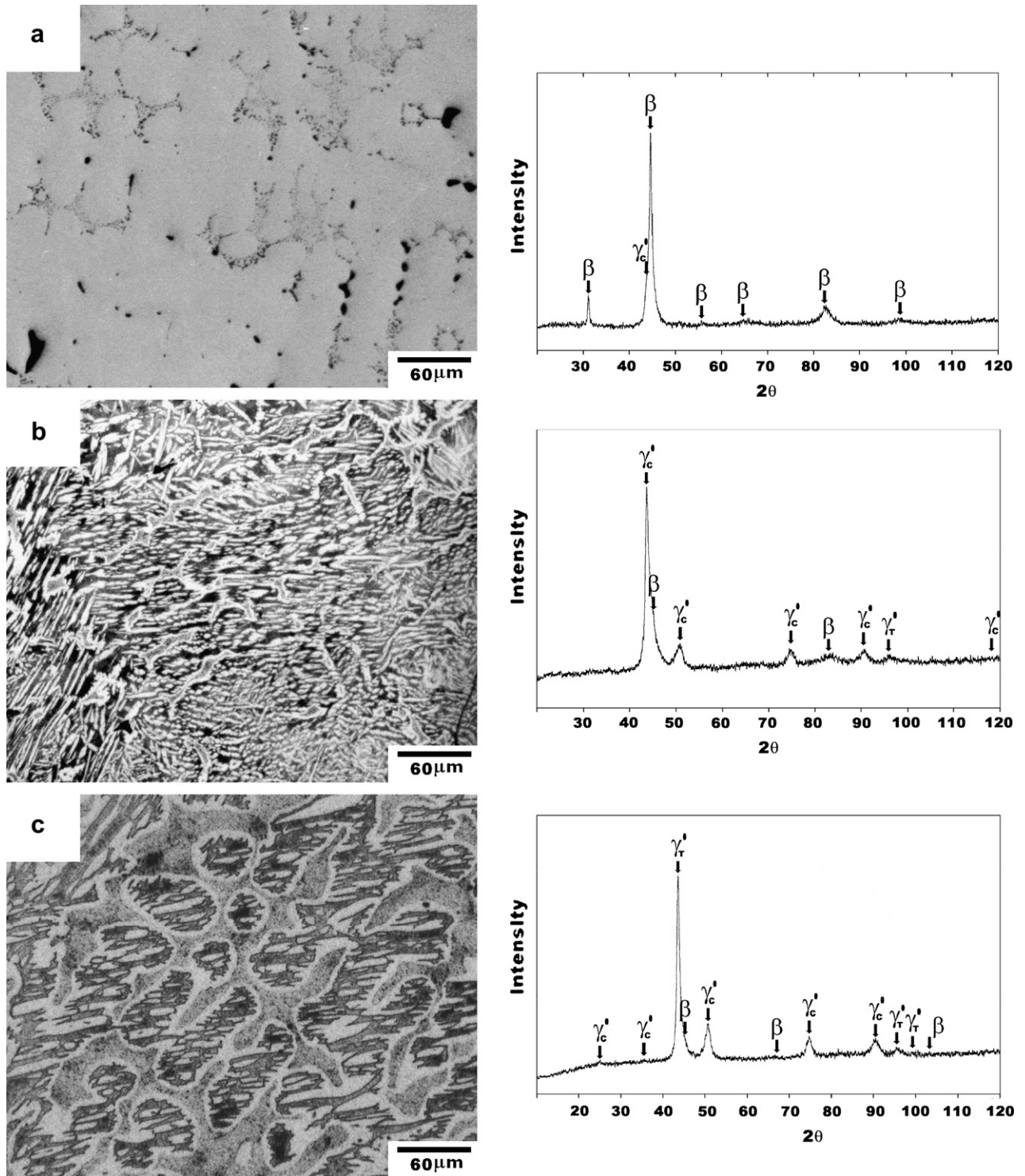


Fig. 2. Observed microstructures and X-ray diffraction patterns obtained from the alloys under study in the as-cast condition: (a) Cu15, (b) Cu20 and (c) Cu25.

grains which are surrounded by a thin film identified as the  $\gamma'_C$  phase, as seen in Figs. 3(b) and 4(c). Similar microstructures were observed by Cheng [13] in binary NiAl alloys but he reported that polygonal grains are constituted by  $\beta$ -NiAl martensite instead of  $\gamma'$ -Ni<sub>3</sub>Al as in the present case. Such difference suggests that Cu additions may suppress the martensitic transformation of the  $\beta$  phase and induce the martensitic transformation of the  $\gamma'$  phase.

Finally, the microstructure of the Cu25 alloy (see Fig. 3(c)) displays equiaxed dendrites of  $\gamma'_C$  with dendrite size less than 6  $\mu\text{m}$  besides the presence of  $\beta$  as secondary phase.

If we look at the ternary Ni–Al–Cu phase diagram in Fig. 1, it is noted that all of the alloys lie in the biphasic field of  $\beta$ -Ni(Al,Cu) plus  $\gamma'$ -(Ni,Cu)<sub>3</sub>Al phases and must show the presence of both phases. This is in good agreement with all the studies in both as-cast and rapid solidification conditions. However, the  $\beta$ -Ni(Al,Cu) phase tends to disappear and its presence is very small in Cu20 and Cu25 rapidly solidified alloys. The tendency of the  $\beta$ -Ni(Al,Cu) phase to disappear is due to the rapid solidification process in which the cooling and the solidification rates are so high,  $\sim 10^6 \text{ K s}^{-1}$ . The extremely



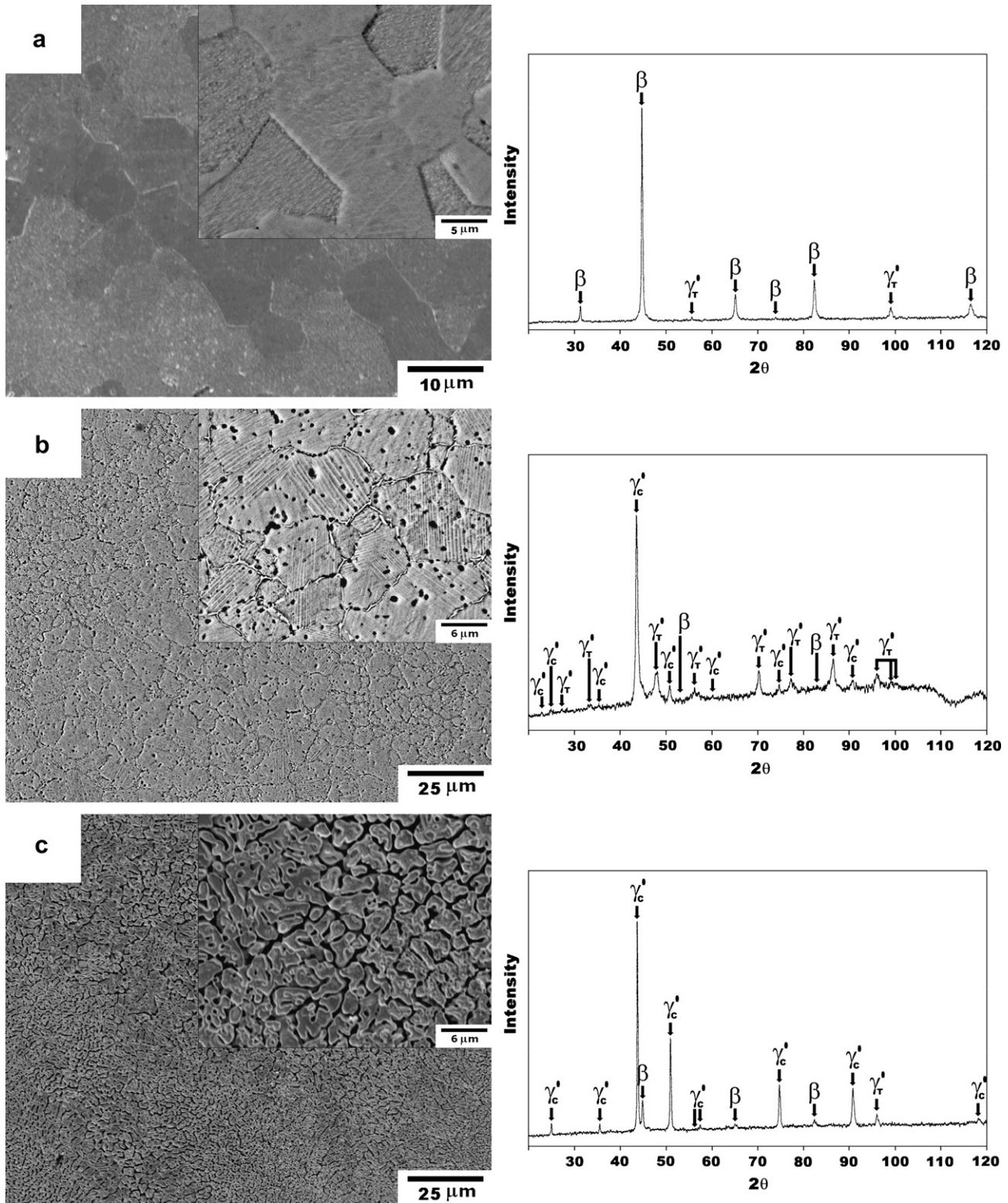
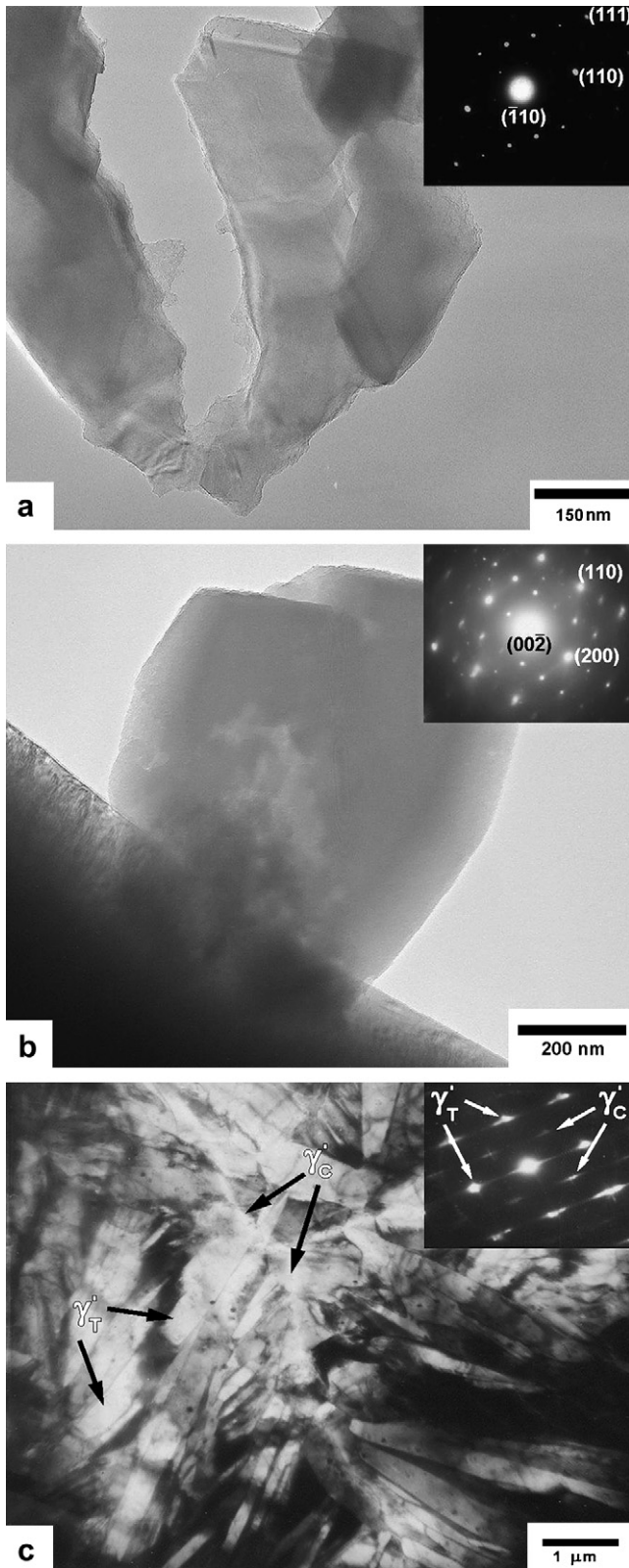


Fig. 3. Observed microstructures and X-ray diffraction patterns obtained from the alloys under study in the rapid solidification condition: (a) Cu15, (b) Cu20 and (c) Cu25.

high heat loss inhibits the diffusion processes limiting, and almost suppressing, the formation of a secondary  $\beta$ -Ni(Al,Cu) phase. This results in an extension of the  $\gamma'$ -(Ni,Cu)<sub>3</sub>Al monophasic field in the alloys Cu20 and Cu25, since these two alloys are closer to the  $\gamma'$ -(Ni,Cu)<sub>3</sub>Al field than to the  $\beta$ -Ni(Al,Cu) field, as it can be seen in Fig. 1.

### 3.2. X-ray diffraction

The presence of the  $\beta$ -(Ni,Cu)Al and  $\gamma'$ -(Ni,Cu)<sub>3</sub>Al phases described above was confirmed by X-ray diffraction tests. However, the last phase showed two different crystal structures, cubic and tetragonal. In order to determine changes in



**Fig. 4.** TEM micrographs showing the tetragonal  $\gamma'$ -(Ni,Cu)<sub>3</sub>Al morphologies observed in the alloys under study: (a) like-plates in the Cu20 as-cast alloy, (b) like-flakes in the Cu25 as-cast alloy, and (c) fine martensite needles in the Cu20 rapidly solidified alloy.

the size of the phase's unit cell, lattice parameter calculations were made using the Bragg's law and the interplanar space values obtained in the X-ray diffraction tests. The results are shown in Table 2.

**Table 2**

X-ray diffraction data obtained from the alloys under study in both as-cast and rapidly solidified conditions

Alloy	Identified phases	Lattice parameter, Å	c/a
Cu15 as-cast	$\beta$ -(Ni,Cu)Al	$a = 2.8671$	–
	$\gamma'_c$ -(Ni,Cu) <sub>3</sub> Al	$a = 3.5777$	–
Cu15 RS <sup>a</sup>	$\beta$ -(Ni,Cu)Al	$a = 2.8608$	–
	$\gamma'_T$ -(Ni,Cu) <sub>3</sub> Al	$a = 3.6753$	0.89799
		$c = 3.3004$	
Cu20 as-cast	$\beta$ -(Ni,Cu)Al	$a = 2.8491$	–
	$\gamma'_c$ -(Ni,Cu) <sub>3</sub> Al	$a = 3.5865$	–
	$\gamma'_T$ -(Ni,Cu) <sub>3</sub> Al	$a = 4.0243$	0.74561
		$c = 3.0005$	
Cu20 RS <sup>a</sup>	$\gamma'_c$ -(Ni,Cu) <sub>3</sub> Al	$a = 3.5984$	–
	$\gamma'_T$ -(Ni,Cu) <sub>3</sub> Al	$a = 3.8443$	0.83565
		$c = 3.2125$	
Cu25 as-cast	$\beta$ -(Ni,Cu)Al	$a = 2.8479$	–
	$\gamma'_c$ -(Ni,Cu) <sub>3</sub> Al	$a = 3.5864$	–
	$\gamma'_T$ -(Ni,Cu) <sub>3</sub> Al	$a = 3.7063$	0.89721
		$c = 3.3253$	
Cu25 RS <sup>a</sup>	$\beta$ -(Ni,Cu)Al	$a = 2.8613$	–
	$\gamma'_c$ -(Ni,Cu) <sub>3</sub> Al	$a = 3.5796$	–

<sup>a</sup> RS – rapidly solidified.

In the same way, to compare experimental and theoretical data, using the parameters in Ref. [14], the concentration dependence of the lattice parameter with Cu concentration was computed. The results are shown in Table 3.

The  $\beta$ -(Ni,Cu)Al is the major phase in the Cu15 alloy as-cast and rapidly solidified, as can be seen in Fig. 2(a). The calculated lattice parameter for the  $\beta$ -(Ni,Cu)Al phase was  $a = 2.867128$  Å and  $a = 2.860821$  Å for the as-cast and rapidly solidified conditions, respectively. In the same alloy,  $\gamma'_c$ -(Ni,Cu)<sub>3</sub>Al exhibits an L1<sub>2</sub> cubic crystal structure ( $\gamma'_c$ ) with lattice parameter  $a = 3.577724$  Å in the as-cast condition. Such a phase changes its crystal structure from cubic to tetragonal (L1<sub>2</sub> → L1<sub>0</sub>) through the rapid solidification process with  $a = 3.675328$  Å and  $c = 3.300400$  Å, the lattice constants for the tetragonal cell.

The Cu20 as-cast alloy shows predominance of  $\gamma'_c$ -(Ni,Cu)<sub>3</sub>Al with  $a = 2.849126$  Å and the same  $\gamma'_c$ -(Ni,Cu)<sub>3</sub>Al phase but of tetragonal structure with  $a = 4.024255$  Å and  $c = 3.000523$  Å in a lesser quantity. Some peaks of  $\beta$ -(Ni,Cu)Al were also detected and the lattice constant for such a phase is  $a = 2.849126$  Å.

For the case of the rapidly solidified Cu20 alloy, the main phase is  $\gamma'_T$  with  $a = 3.844333$  Å and  $c = 3.212544$  Å, present inside the polygonal grains which are surrounded by a thin film of  $\gamma'_c$  phase with  $a = 3.598430$  Å. One peak of  $\beta$ -(Ni,Cu)Al phase was detected, indicating an almost total suppression of the formation of the  $\beta$ -(Ni,Cu)Al phase due to the rapid solidification process.

Finally,  $\gamma'_c$  seems to be the main phase in the Cu25 as-cast alloy, followed by  $\gamma'_T$ . Calculated lattice parameters for the tetragonal and the cubic phases are  $a = 3.706284$  Å,  $c = 3.325327$  Å and  $a = 3.580551$  Å, respectively.

**Table 3**

Computed lattice parameters ( $a$ ) for the  $\beta$ -Ni(Al,Cu) phase as a function of the Cu concentration in the Ni-rich alloys

Cu content, at.%	$a$ (Å) for $\beta$ -Ni(Al,Cu)
0	2.8867
5	2.8789
10	2.872
15	2.8656
20	2.8598
25	2.8545



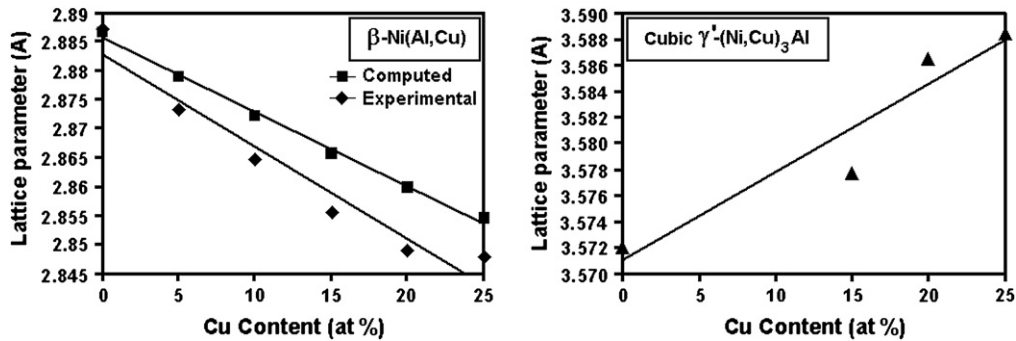


Fig. 5. Variation of the lattice parameter  $a$  for the cubic  $\beta$ -Ni(Al,Cu) and  $\gamma'$ -(Ni,Cu)<sub>3</sub>Al phases as a function of the Cu content in the alloy.

On the other hand, in the Cu25 rapidly solidified alloy,  $\gamma'_T$  almost disappears and only one peak was detected by the X-ray beam. The  $\gamma'_C$  with  $a = 3.579642$  is the main phase in this alloy according to the X-ray diffraction patterns, followed by the  $\beta$ -(Ni,Cu)Al phase. The calculated lattice parameter for the  $\beta$ -(Ni,Cu)Al phase is  $a = 2.861302$  Å. In a general way, it is observed that the lattice parameter of the  $\beta$ -(Ni,Cu)Al phase in the as-cast alloys tends to decrease while the concentration of Cu increases, relative to the  $a = 2.887$  Å value reported for the binary NiAl at the stoichiometric composition [15] (see Fig. 5). At this point, it is important to mention that Bozzolo et al. [16,17] have performed extensive work regarding the site occupancy of ternary elements added to the NiAl intermetallic compound. In recent papers, Bozzolo et al. [16,17] reported that according to the BFS method, Cu atoms prefer the occupancy of Ni sites better than Al sites in Al-rich NiAl compositions. On the other hand, in Ni-rich NiAl compositions, Cu atoms prefer the occupancy of Al sites better than Ni sites. In the present work, the decrease of the lattice parameter mentioned above for  $\beta$ -Ni(Al,Cu) is due to the fact that with the increase in the Cu content there is a decrease of Al in the alloy and, since the alloys are Ni-rich, Cu atoms substitute for Al atoms occupying their sites ( $\text{Cu}_{\text{Al}}$ ). Given that the Cu atoms are about 10.75% smaller than the Al atoms ( $r_{\text{atCu}} = 1.278$  Å;  $r_{\text{atAl}} = 1.432$  Å), a decrease in the lattice parameter is observed confirming the theoretical information reported by Bozzolo et al. [18], see Fig. 5,  $\beta$ -Ni(Al,Cu).

In the same alloys, cubic  $\gamma'$ -(Ni,Cu)<sub>3</sub>Al exhibits an increase in the lattice parameter, as seen in Fig. 5, due to the substitution of Cu atoms in Ni sites ( $\text{Cu}_{\text{Ni}}$ ), since the Cu atom is slightly (2.74%) bigger than Ni ( $r_{\text{atCu}} = 1.278$  Å;  $r_{\text{atNi}} = 1.243$  Å). In this case, the lattice parameters of the cubic  $\gamma'$ -(Ni,Cu)<sub>3</sub>Al in the macroalloyed alloys are bigger than that of  $a = 3.572$  Å reported for the binary  $\gamma'$ -Ni<sub>3</sub>Al [19].

Regarding the tetragonal  $\gamma'$ -(Ni,Cu)<sub>3</sub>Al, there are no reports in the literature concerning this ternary phase except for the 21-8

JCPDS card of the binary tetragonal  $\gamma'$ -Ni<sub>3</sub>Al. Such a binary phase is the result of a tetragonal distortion  $L1_2 \rightarrow L1_0$  produced by quenching the cubic  $\gamma'$ -Ni<sub>3</sub>Al phase from 1300 °C. It has been reported [20,21] that such distortion can be produced by a point defect such as a vacancy or an antisite atom in the top and bottom faces of the cube, shown in Fig. 6. At this point, the cubic  $\gamma'$ -Ni<sub>3</sub>Al possesses an  $L1_2$  type unit cell in which the Ni atoms are located in the faces of the cube and the Al atoms in the corners. If two Al atoms substitute for two Ni atoms located in opposite faces of this cell, a tetragonal distortion as the one shown in Fig. 6 will occur. In the present case, given that Cu atoms prefer substitution for Ni better than Al in the Ni<sub>3</sub>Al intermetallic phase [22], the addition of Cu produces the formation of tetragonal martensite by the substitution of Cu atoms in Ni sites ( $\text{Cu}_{\text{Ni}}$ ) located in opposite faces of the cube.

In the Cu20 and Cu25 alloys as-cast and rapidly solidified, the tetragonal  $\gamma'$ -(Ni,Cu)<sub>3</sub>Al was formed, being the major phase in the rapidly solidified Cu20 alloy. This indicates that at least in the alloys as-cast, Cu can induce a partial transformation of cubic  $\gamma'$ -(Ni,Cu)<sub>3</sub>Al into a tetragonal  $\gamma'$ -(Ni,Cu)<sub>3</sub>Al, and it can be obtained from the casting without the need for a subsequent tempering treatment to produce the martensitic structure as reported for the binary  $\gamma'$ -Ni<sub>3</sub>Al. In addition, the rapid solidification process produces a martensitic transformation of  $\gamma'$ -(Ni,Cu)<sub>3</sub>Al refining the martensite from plates observed in the as-cast state to fine needles observed in the rapidly solidified alloys.

An anomalous behaviour of binary  $\gamma'$ -Ni<sub>3</sub>Al, which consists of an increase of the stress flow as the temperature rises from room temperature up to 700 °C, has been reported. Several researchers [23] have explained the phenomenon in terms of lattice defects such as splitting of screw dislocations and antiphase boundary energies. However, Numakura et al. [20] proposed an alternative mechanism for the mentioned anomalous phenomenon, in which the stress-induced redistribution of point defects on the Ni sublattice sites is responsible for this so-called "anelastic relaxation effect". Since a point defect on an Ni sublattice site constitutes a tetragonal defect in the Ni<sub>3</sub>Al system, a substitutional atom or vacancy can induce an anelastic relaxation.

In the present work we assume that Cu atoms substitute for Ni atoms observing a tetragonal distortion which we attribute mainly to an abrupt cooling, instead of a stress-induced mechanism, as proposed by Numakura.

#### 4. Conclusions

Cu additions to the Ni-rich NiAl intermetallic compound produce abrupt changes in the microstructural morphology of the as-cast alloys, from columnar dendrites in alloys with Cu contents lower than 15 at.%, to plate microstructures in alloys with Cu contents higher than 15 at.%. Furthermore, Cu additions would

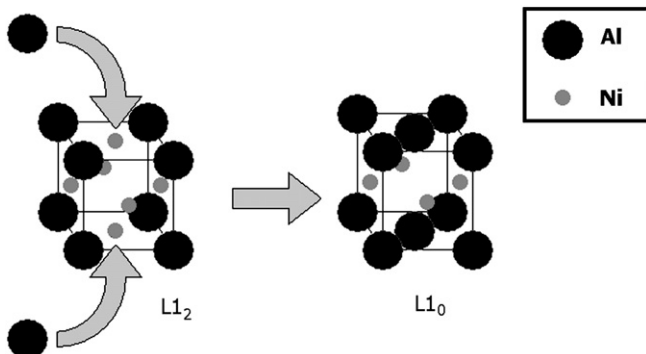


Fig. 6. Allotropic forms for the Ni<sub>3</sub>Al intermetallic compound.

suppress the martensitic transformation of the  $\beta$  phase and induce an almost total martensitic transformation of the  $\gamma'$  phase through a rapid solidification process.

The  $\gamma'$ -(Ni,Cu)<sub>3</sub>Al martensitic phase observed in the current work, is the result of a tetragonal distortion produced by the addition of Cu atoms replacing and occupying Ni sites in the  $\gamma'$ -Ni<sub>3</sub>Al crystal lattice.

$\gamma'$ -Ni<sub>3</sub>Al intermetallic compound exhibits a flow stress anomalous temperature dependence which according to Numakura, is related to an “anelastic relaxation effect” produced by a tetragonal distortion of the  $\gamma'$ -Ni<sub>3</sub>Al phase. Numakura suggests that the ARE is caused by the stress-induced redistribution of point defects i.e. substitution of Al atoms in Ni sites. In the present work the substitutional atoms are Cu instead of Al, and the mechanism is not stress-induced but an abrupt cooling.

Cu addition decreases the lattice parameter values of  $\beta$ -Ni(Al,Cu) which is due to the occupancy of Cu atoms in Al sites. These experimental results confirm the theoretical data reported by Bozzolo et al.

### Acknowledgements

The authors would like to thank Mr. Anselmo González-Trujillo, G. Lara, M.S., L. Baños, B. Eng, and I. Puente, B. Eng. for technical assistance.

### References

- [1] Pope DP, Darolia R. In: Westbrook JH, editor. Applications of intermetallic compounds. MRS Bulletin, vol. 21; 1996. p. 26.
- [2] Aoki K, Ishikawa K, Masumoto T. Mater Sci Eng A 1995;192/193:316–23.
- [3] Darolia R. J Met 1991;43(3):44–9.
- [4] Schulson EM, Xu Y. Acta Mater 1997;vol. 45(8):3491–4.
- [5] Chiba A, Hanada S, Watanabe S. Mater Sci Eng A 1992;152:108–13.
- [6] Ishida K, Kainuma R, Ueno N, Nishizawa T. Metall Trans A 1991;22:441–6.
- [7] Chun-Huei T. Intermetallics 2001;9:1085–7.
- [8] Kim SH, Oh MH, Wee DM. Mater Sci Forum 2003;426:1813.
- [9] Kim SH, Kim MC, Lee JH, Oh MH, Wee DM. Mater Sci Eng A 2002;329:668.
- [10] Subramanian PR, Mendiratta MG, Miracle DB. Metall Trans A 1994;25:2769.
- [11] Kainuma R, Imano S, Otani H, Ishida K. Intermetallics 1996;4:37.
- [12] Bradley AJ, Lipson H. Proc R Soc London Ser A 1938;167:421–438.
- [13] Cheng T. J Mater Sci 1995;30:2877–87.
- [14] Bozzolo G, Mosca H, Wilson A, Noebe RD, Garces JE. Metall Trans B 2002;33:265.
- [15] Noebe RD, Bowman RR, Nathal MV. Int Mater Rev 1993;38:193.
- [16] Bozzolo G, Noebe RD, Garces JE. Scripta Mater 2000;42:403–8.
- [17] Bozzolo G, Noebe RD, Honey F. Intermetallics 2000;8:7–18.
- [18] Bozzolo GH, Noebe RD, Amador Carlos. Intermetallics 2002;10:149–59.
- [19] JCPDS–ICDD, card 9-97 (cubic Ni<sub>3</sub>Al), card 21-8 (tetragonal Ni<sub>3</sub>Al).
- [20] Numakura H, Kurita N, Koiwa M. Philos Mag A 1999;79:943–53.
- [21] Barret CS, Massalski TB. The structure of metals and alloys. Structure of metals. Crystallographic methods, principles and data. 3rd revised ed. Oxford, New York, Seoul, Tokyo: Pergamon Press; 1980. p. 272–3.
- [22] Sauthoff G. Intermetallics. Weinheim, New York, Basel, Cambridge, Tokyo: VCH; 1995. p. 40.
- [23] Sauthoff G. Intermetallics. Weinheim, New York, Basel, Cambridge, Tokyo: VCH; 1995. p. 41–3.